

## Supplementary Materials

### *S1: MaxEnt Model Complexity*

The default setting in Maxent can determine which suitable feature type to use based on the number of presence samples in the model. The followings are the functions of the feature types used in this study<sup>1</sup>:

- i. Linear features ensure that the mean value of the continuous environmental variable at a location where the species is predicted to occur approximately matches the mean value where it is observed.
- ii. Quadratic feature constrains the variance in an environmental variable where the species is predicted to match the observation.
- iii. Product features constrain the covariances of the environmental variables where the species is predicted to match the observation.
- iv. Threshold features make continuous predictors binary by distinguishing the value below the threshold equal to 0 and above the threshold equal to 1.
- v. Hinge feature is like the threshold, except a linear function is utilized instead of a step function.

### *Performance Metrics*

The calibration accuracy was determined based on the Expected Calibration Error (ECE) and Maximum Calibration Error (MCE). We also used the Continuous Boyce Index (CBI) as an additional assessment tool because the Boyce indices could provide insight into the model's robustness and deviation from randomness<sup>2</sup> or simply means the model transferability to a different geographical area. The CBI measures the Spearman rank correlation coefficient between predicted-to-expected ratio (F) against the mean habitat suitability of each bin using moving window<sup>3</sup>. Besides, the ECE is the best performing metric according to previous study for model selection by far (in the case of Maxent model) and the perfect model has  $ECE = 0$ <sup>4</sup>.

## Optimized Maxent Model Performances

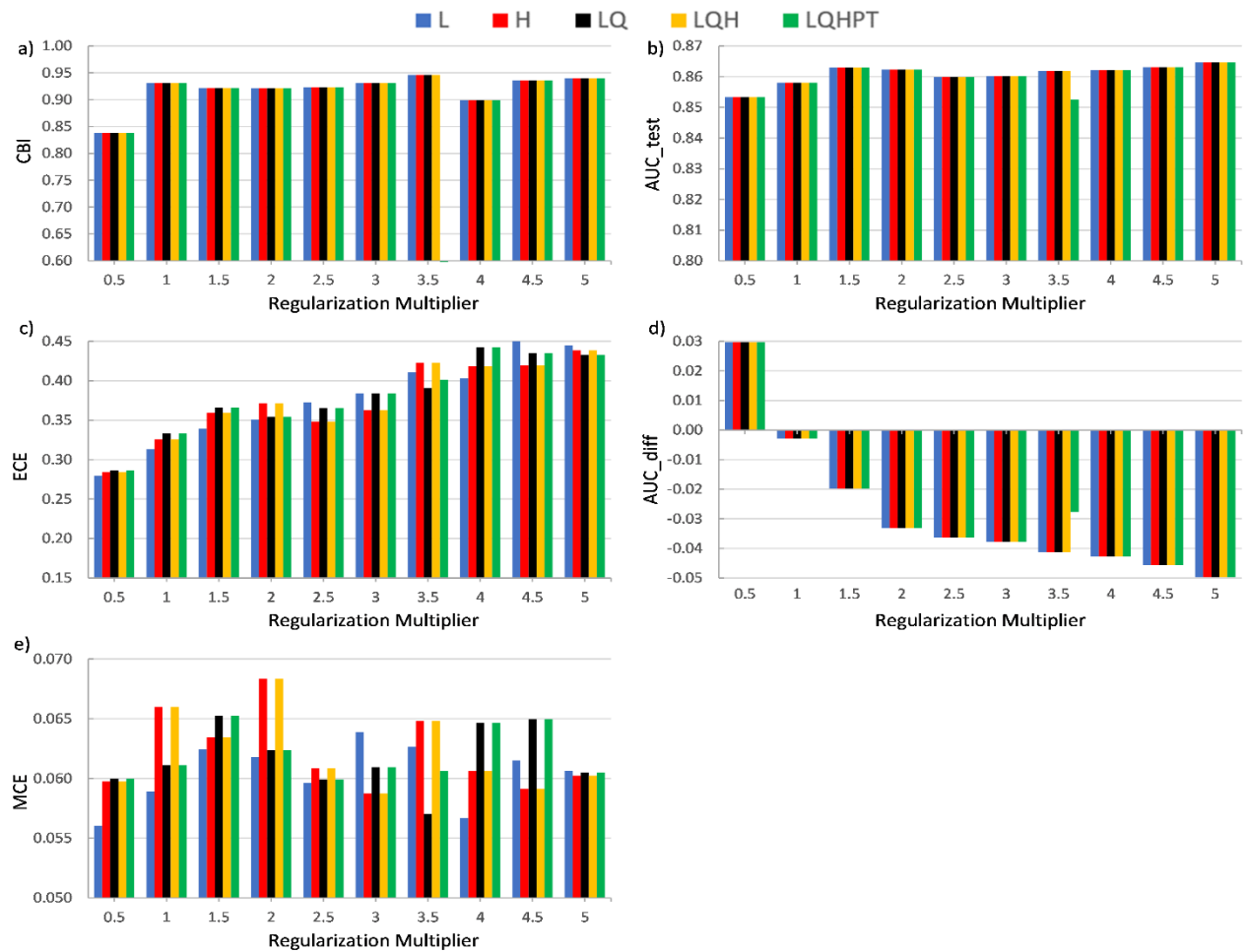


**Figure S1.** MaxEnt models tuning performances with various features combination (L, H, LQ, LQH and LQHPT) and regularization multiplier (rm). Plots (a), (c) and (e) represent the calibration accuracy of the models, which are continuous Boyce Index (CBI), expected calibration error (ECE) and maximum calibration error (MCE), respectively. The discrimination accuracy was assessed using AUC\_test (b) and AUC\_diff (d).

The AUC\_test showed little difference between the models with various feature types, but under  $rm=3.5$ , the model with LQHPT features combination showed a significantly lower AUC\_test than the other models. Figure S1 (d) shows significant negative gains in the AUC\_diff trend with the increasing rm values except for  $rm=0.5$ , which is significantly overfitted. Calibration accuracies shown in Figures S1(a), (c) and (e) suggest that the combination of each feature give about the same performance in CBI under different regularization values, with the lowest CBI was noted when  $rm=0.5$  for all features combination. The ECE plot showed an increasing trend of ECE values with increasing rm values, but the values vary under different feature types. Employing features combination of H and LQH resulted in the same ECE and MCE. Similarly, under features LQ and LQHPT, the model generated the same ECE and MCE, but these values are different for different values of regularization (see ECE,  $rm=3.5$  and  $4.5$ ). A regularization value of 1 showed a better model performance with low ECE and high CBI values. As shown in Figure S1 (d), the AUC\_diff trend decreases (negative) with increasing rm values, suggesting that the higher rm values would result in a better AUC from test data. However, a higher rm value will result in high ECE, which is not suitable for the optimal model.

## S2: Local Climate Trend

**Figure S2** depicted the local climate of Setiu, Kuala Terengganu (K. Trg) and Marang districts. The World Weather Online (WWO) website was used to collect statistics on average precipitation and temperature, which were reliably sourced from a global weather satellite, a world meteorological organization, and a global telecommunication system<sup>5</sup>. These three districts showed a different trend in the Monthly Average Low Temperature (MALT). The MALT trend for Setiu shows a consistent temperature of about 25°C from April to October and decreases to about 23°C from November to February. While for Marang, the temperature is about 25°C from July to December. In K. Trg, the MALT is higher than in the other two districts. However, all the districts depict almost the same trend, which recorded lower temperatures from January to March, then increased temperature during April or May, and decreased in November. Similar patterns are observed for the Monthly Average High Temperature (MAHT), where the temperature is lowest in January, then increasing until April or May, but then decreased again from October to December. When we compare with the monthly average precipitation (MAP) graph, the trends depicted high precipitation from October to January, then declined in February and varies below 300 mm during March until September except for Setiu, where there is a peak during May and slightly higher during August to October.

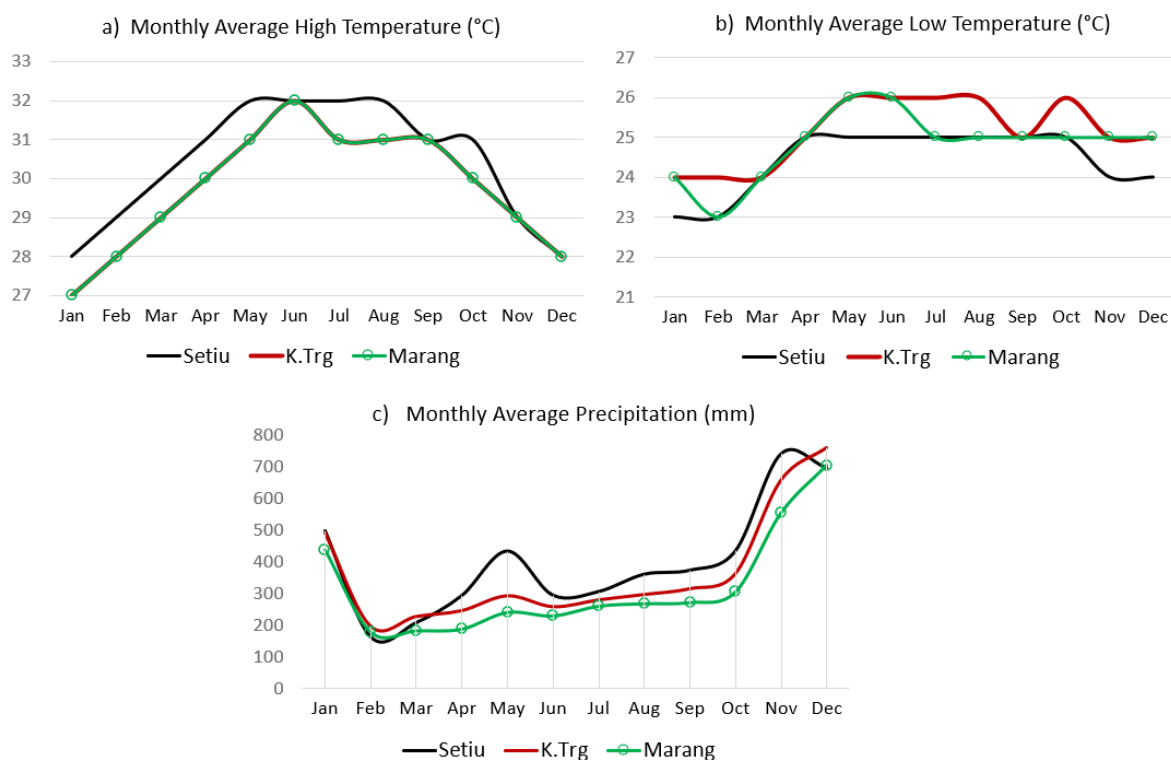


**Figure S2.** Local climate of Setiu, Kuala Terengganu and Marang districts. The (a) monthly average high temperature, (b) monthly average of low temperature and (c) monthly average precipitation (WorldWeatherOnline, 2019).

## S3: Global Climate Models Evaluation Method

A study has reviewed the performances of 40 Global Climate Models (GCMs) <sup>6</sup>. The study performed 19 performance metrics as listed in Table S3. Out of 19, 11 performance metrics are computed for land only, sea only, and both land and sea for the 40-year period of 1960–1999 which the observation datasets

are available. Another eight-performance metrics evaluate the long-term performance of simulated climatological temperature and precipitation for the 99-year period of 1901 to 1999 for land only. The **total error** (E) of a global climate model  $j$  is computed as follows:

$$E_j = \sum_{i=1}^n R_{i,j} \quad (\text{Eq.1})$$

$$R_{i,j} = (A_{i,j} - A_{i,\min}) - (A_{i,\max} - A_{i,\min}) \quad (\text{Eq.2})$$

$$A_{i,j} = |O_i - S_{i,j}| \quad (\text{Eq.3})$$

Where,

$A_{i,j}$  is the absolute error for each performance metric  $i$  and each global climate model  $j$ ,

$O_i$  performance metric  $i$  of observations,

$S_{i,j}$  simulated performance metric  $i$  of the global climate model  $j$ ,

$R_{i,j}$  is the relative error for each performance metric  $i$ , and

$n$  is total number of performance metrics.

**Table S1.** List of Performance metrics performed in the evaluation of 40 GCMs. Summarized from study by Kamworapan and Surussavadee (2019).

No	Performance metrics
1	Mean annual temperature
2	Mean annual precipitation
3	Mean diurnal temperature range
4	Mean seasonal cycle amplitude of temperature
5	Mean seasonal cycle amplitude of precipitation (precipitation difference between wettest and driest months)
6	Correlation coefficient between simulated and observed mean temperature
7	Correlation coefficient between simulated and observed mean precipitation
8	Standard deviation of mean temperature
9	Standard deviation of mean precipitation
10	Root mean squared error of mean temperature
11	Root mean squared error of mean precipitation
12	Variance of annual average temperature
13	Mean-normalized standard deviation of 99-year annual precipitation
14	Root mean squared error of annual average temperature
15	Root mean squared error of annual precipitation
16	Linear trend of annual average temperature
17	Linear trend of annual precipitation
18	Correlation coefficient of the cold season temperature mean and Niño3.4 index
19	Correlation coefficient of the cold season precipitation and Niño3.4 index

## References

- (1) Phillips, S. J.; Dudík, M. Modeling of Species Distributions with Maxent: New Extensions and a Comprehensive Evaluation. *Ecography (Cop.)*. **2008**, *31* (2), 161–175. <https://doi.org/10.1111/j.0906-7590.2008.5203.x>.
- (2) Boyce, M. S.; Vernier, P. R.; Nielsen, S. E.; Schmiegelow, F. K. A. Evaluating Resource Selection Functions. *Ecol. Modell.* **2002**, No. 157, 281–300.
- (3) Hirzel, A. H.; Le Lay, G.; Helfer, V.; Randin, C.; Guisan, A. Evaluating the Ability of Habitat Suitability Models to Predict Species Presences. *Ecol. Modell.* **2006**, *199* (2), 142–152. <https://doi.org/10.1016/j.ecolmodel.2006.05.017>.
- (4) Warren, D. L.; Matzke, N. J. Evaluating Presence-Only Species Distribution Models with Discrimination Accuracy Is Uninformative for Many Applications. *J. Biogeogr.* **2020**, *47*, 167–180. <https://doi.org/10.1111/jbi.13705>.
- (5) WorldWeatherOnline. Current weather report available at: <https://www.worldweatheronline.com/kuala-terengganu-weather-averages/terengganu/my.aspx> (accessed Apr 14, 2021).
- (6) Kamworapan, S.; Surussavadee, C. Evaluation of CMIP5 Global Climate Models for Simulating Climatological Temperature and Precipitation for Southeast Asia. *Adv. Meteorol.* **2019**, *2019*. <https://doi.org/10.1155/2019/1067365>.